p-type Bi0.4Sb1.6Te3 nanocomposites with enhanced figure of merit

Fan, Shufen; Zhao, Junnan; Guo, Jun; Yan, Qingyu; Ma, Jan; Hng, Huey Hoon

2010

Fan, S., Zhao, J., Guo, J., Yan, Q., Ma, J., & Hng, H. H. (2010). p-type Bi0.4Sb1.6Te3 nanocomposites with enhanced figure of merit. Applied physics letters, 96(18), 182104-.

https://hdl.handle.net/10356/90570

https://doi.org/10.1063/1.3427427

p-type $Bi_{0.4}Sb_{1.6}Te_3$ nanocomposites with enhanced figure of merit

Shufen Fan,[1] Junnan Zhao,[1] Jun Guo,[1] Qingyu Yan,[1] Jan Ma,[2] and Huey Hoon Hng[1,a)]
[1]*School of Materials Science and Engineering, Nanyang Technological University, Singapore 639798*
[2]*Temasek Laboratories, Nanyang Technological University, 50 Nanyang Drive, Singapore 637553*

(Received 23 March 2010; accepted 16 April 2010; published online 6 May 2010)

We report enhanced figure of merit, ZT, in p-type $Bi_{0.4}Sb_{1.6}Te_3$ nanocomposites fabricated by a rapid and high throughput method of mixing nanostructured $Bi_{0.4}Sb_{1.6}Te_3$ particles obtained through melt spinning with micronsized particles obtained via solid state reaction. Due to effective scattering of phonons over a wide wavelength spectrum, low thermal conductivity, and moderately good power factor were obtained in the nanocomposites to achieve ZT above 1.5 at room temperature. A maximum ZT of 1.80 was attained at 43 °C for the nanocomposite consisting 40 wt % nanoinclusions. This was a 56% increment over the bulk sample, and the highest ZT reported for Bi_2Te_3-based materials. © *2010 American Institute of Physics*. [doi:10.1063/1.3427427]

The ever increasing energy demand and growing global concern over the environmental impact of CO_2 emission pave the way for the transition from fossil fuels to sustainable energy. Moreover, with over 70% of the energy generated from primary energy sources wasted as dissipated heat,[1] heat scavenging is expected to play a significant role in improving sustainability. Thermoelectric (TE) devices can directly convert between heat and electrical energy, and have long term stability and are CO_2 emission free.[2] However, its present usage is limited to niche applications[3] due to its low conversion efficiency. The efficiency of TE materials is governed by the dimensionless figure of merit, ZT and is defined as $ZT=S^2\sigma T/\kappa$, where S, σ, κ, and T are the Seebeck coefficient, electrical conductivity, thermal conductivity, and absolute temperature, respectively. These parameters are interdependent in bulk materials, making it difficult to optimize the ZT of bulk TE materials. On the other hand, these parameters have been shown theoretically[4] and demonstrated by Venkatasubramanian *et al.*[5] and Harman *et al.*[6] separately that in low dimensional materials, the parameters can be varied more independently. High ZT values of 2.4 and 1.6 were achieved in Bi_2Te_3/Sb_2Te_3 superlattices and $PbSe_{0.98}Te_{0.02}/PbTe$ quantum dots, respectively, at 300 K, owing to a large decrease in thermal conductivity. However, fabrication processes of such low dimensional materials are expensive and have low throughput. Studies have shown that reduced thermal conductivity can also be obtained in materials with high density of interfaces, which can be present in any geometry.[7] The presence of nanostructures with size smaller than the phonon mean free path will greatly enhance phonon scattering by scattering the mid and long wavelength phonons, and hence result in a marked decrease in the thermal conductivity.[8] Hence, a more promising approach is to fabricate nanocomposites which retain the high density of interfaces and can be produced using scalable and inexpensive processes. Nanostructured bulk with improved ZT has been demonstrated recently via high energy ball milling followed by hot pressing. Improved ZT of 1.4 at 100 °C and 1.3 at 900 °C were obtained in BiSbTe (Ref. 9) and SiGeP (Ref. 10) bulk nanostructures, respectively. Apart from high energy ball milling, nanoparticles for nanocomposites were also produced via chemical synthesis.[11–15] However, these processing methods are either time consuming or has low yield. On the other hand, melt spinning is able to produce large quantity of nanostructured materials within a short time span. Various bulk nanostructured TE materials have been prepared via melt spinning and have also showed improved ZT.[16–18] In this work, $Bi_{0.4}Sb_{1.6}Te_3$ nanocomposites with enhanced ZT were fabricated via a high throughput and scalable process which incorporates melt spinning to obtain the nanophase, followed by mixing with the bulk phase, and finally densification via hot pressing.

Bismuth needles (99.99%), tellurium (99.8%), and antimony powder (99.5%) were used as starting materials to prepare p-type $Bi_{0.4}Sb_{1.6}Te_3$ ingots via solid-state synthesis. The powder mixture was loaded into a quartz ampoule, sealed under vacuum at 10^{-3} Pa, and then heated at 800 °C for 10 h. The ingots were then used as precursors for the preparation of the nanocomposites. The ingot served two purposes here, the first as the bulk phase for the nanocomposites and second as precursor for the preparation of the nanoinclusions. The nanoinclusions were prepared via melt spinning from the ingot with a linear speed of 60 Hz and working distance of 0.5 mm. The composite mixture was obtained by mixing the bulk phase with various amount of nanoinclusions (0, 10, 20, and 40 wt %) using the horizontal ball mill, and then hot pressed at 450 °C, 50 MPa for 30 min in an argon environment to obtain the bulk nanocomposites. The thermoelectric properties of the nanocomposites were compared against the 0 and 100 wt % samples to elucidate the effect of adding nanoinclusions on the TE properties.

High-resolution transmission electron microscope (HRTEM) (JEOL, JEM-2100F) was used to analyze the microstructures and energy dispersive x-ray spectroscopy for elemental composition analysis. Electrical conductivity and Seebeck coefficient were measured using a commercial instrument [ULVAC-Riko, ZEM-3 (M8)] over the temperature range of 25–250 °C in helium environment. The thermal diffusivity, D, was measured using the laser flash method (Netzsch, LFA 447). The specific heat, C_p, was determined from the comparison method with a standard sample tested under the same conditions. The density, ρ, was measured by

a)Author to whom correspondence should be addressed. Electronic mail: ashhhng@ntu.edu.sg. Tel.: +65 6790 4140.

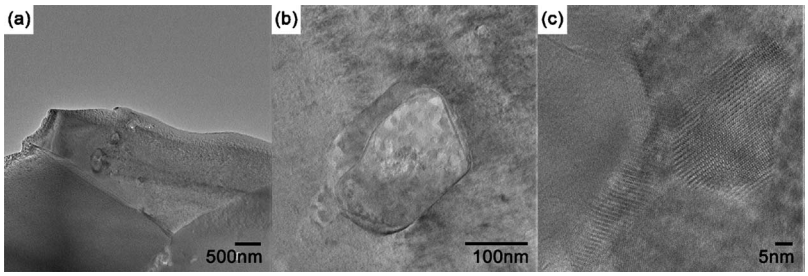

FIG. 1. TEM images of typical nanocomposite showing (a) nanograins embedded in micronsized grains, (b) magnified image of the nanograin, and (c) nanoprecipitate embedded within the nanograin.

Archimedes method and thermal conductivity, κ, calculated using the equation, $\kappa = D \times \rho \times C_p$. The lattice thermal conductivity, κ_L, was calculated from the Wiedemann–Franz relation, $\kappa_L = \kappa - \kappa_E$, where $\kappa_E = L\sigma T$ is the electronic thermal conductivity, $L = 2.0 \times 10^{-8}$ V^2/K^2 is the Lorentz number for a degenerate semiconductor,[19] σ is the electrical conductivity, T is the temperature in Kelvin, and κ_L is the lattice thermal conductivity.

The TEM images in Fig. 1 represent the typical microstructures observed in the nanocomposite samples. Figure 1(a) shows a typical bright field image showing the distribution of the micronsized and nanosized grains within the nanocomposite. The nanosized grains were less than 200 nm and consisted of nanoprecipitates that were in the order of few tens of nanometers [Fig. 1(b)]. Figure 1(c) shows the HRTEM image of a 15 nm Sb-rich nanoprecipitate with diffused boundaries embedded in it. Similar nanoprecipitates were also observed in the structure study[20] of nanostructured bulk BiSbTe, where the authors attributed the reduction in thermal conductivity to efficient phonon scattering due to the presence of a wide range of random-sized particles.

Marked reduction in the thermal conductivity ranging from 30%–47% was observed in the nanocomposites as well as the 100 wt % (nanophase) samples, and the thermal conductivity decreased with increasing weight percent nanoinclusions [Fig. 2(a)]. The thermal conductivity of the nanocomposites was also observed to increase at a slower rate with increasing temperature as compared to the 0 wt % sample (bulk). In bulk materials, mid and long wavelength phonons are not strongly affected by the scattering events, and are hence still able to transport heat. However, due to the high density of interfaces and grain boundaries present in the nanocomposites and 100 wt % nanosample, the scattering of phonons across a broad wavelength spectrum was enhanced. This suppressed the lattice thermal conductivity of the nanocomposites significantly by 66% as compared to the bulk. Consequently, the nanocomposites exhibited an average low κ_L of ~ 0.16 $W\ m^{-1}\ K^{-1}$ at room temperature. This value lies within the minimum lattice thermal conductivity limit defined by Slack, which is in the range of $0.1-0.2$ $W\ m^{-1}\ K^{-1}$. Apart from the reduction in the lattice thermal conductivity, electronic thermal conductivity also underwent moderate reduction. For the 40 wt % NC, the room temperature electronic thermal conductivity was reduced by 27% to 0.50 $W\ m^{-1}\ K^{-1}$ as determined via the Wiedemann–Franz relation. Conversely, the interface scattering also affects the electron transport in the nanocomposites as the carriers are also scattered by the grain boundaries. As a result, this may be an obstruction to achieving improved ZT in nanocomposites. However, this problem can be coun-

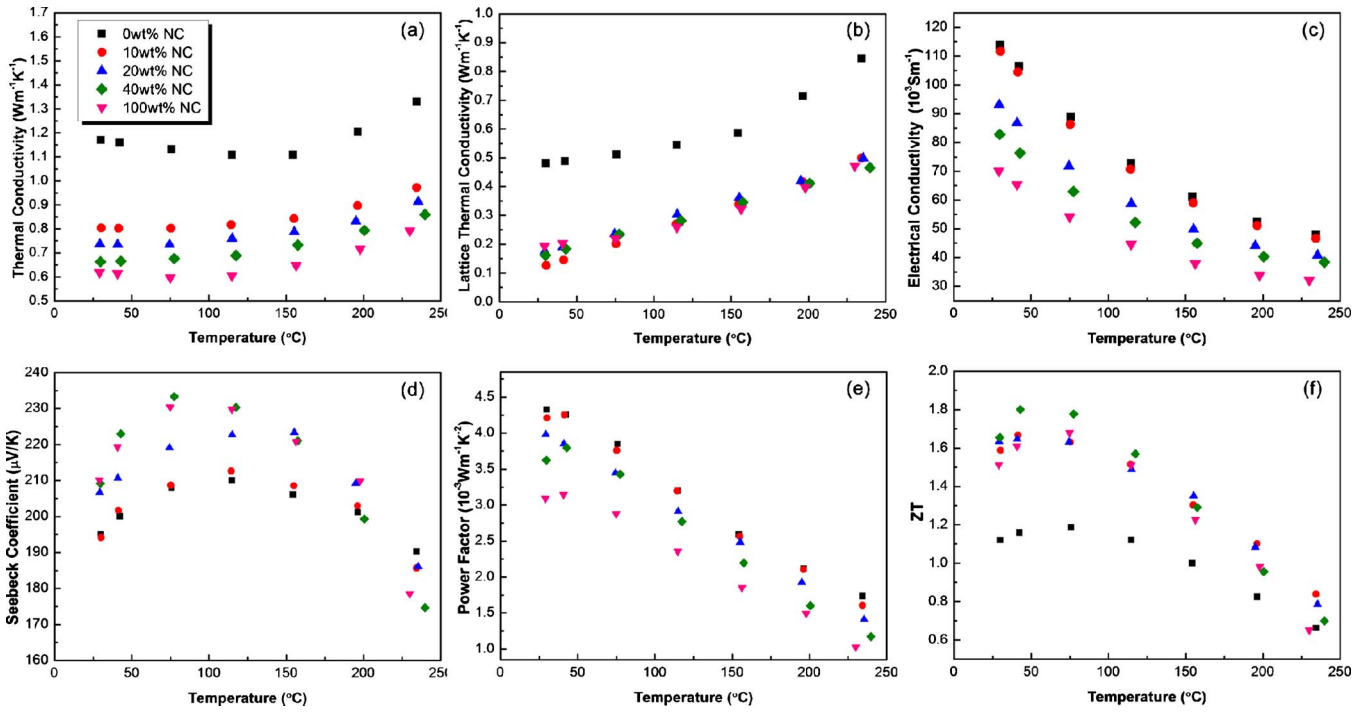

FIG. 2. (Color online) Thermoelectric properties of the nanocomposites with various weight percent nanoinclusions. (a) Thermal conductivity, (b) lattice thermal conductivity, (c) electrical conductivity, (d) Seebeck coefficient, (e) power factor, and (f) ZT.

tered by using the same material as that used for the bulk phase for the nanoinclusions to reduce the band edge offset,[8] and hence preventing a drastic decrease in the electrical conductivity. As shown in Fig. 2(c), the electrical conductivity of the nanocomposites decreased with increased weight percent of nanoinclusions due to the increased number of grain boundaries and the presence of more scattering centers which reduced the carrier mobility. The electrical conductivity of the nanocomposites decreased slower at the higher temperature range, and eventually became comparable in magnitude to the 0 wt % sample. The effect of reduced mobility due to grain boundary scattering also aids in the scattering of electrons with energies less than the barrier height. As shown in Fig. 2(d), the Seebeck coefficient of the nanocomposites increased with increasing weight percent nanoinclusions, with the 40 wt % NC exhibiting similar Seebeck coefficient to the 100 wt % NC ($\sim$230 μV/K). This shows that the increment is due to the addition of nanoinclusions and that through energy filtering, low energy electrons are preferentially scattered, minimizing their contributions to transport properties, and increases the Seebeck coefficient. As a result of the slight improvement in Seebeck coefficient and moderate decrease in electrical conductivity, the nanocomposites were able to maintain a moderately high power factor with respect to the 0 wt % sample [Fig. 2(e)]. Hence, combining the low thermal conductivity that was maintained over a wide temperature range and moderately high power factor exhibited by the nanocomposites, the maximum ZT values of all the nanocomposites were over 1.6 [Fig. 2(f)] and ZT$>$1.0 were maintained for temperatures up to 200 °C. Also, as the decrease in electrical conductivity was much less than the decrease in thermal conductivity, a maximum ZT of 1.8 was obtained at 43 °C for the 40 wt % NC which was a 56% improvement over the 0 wt % NC sample.

In conclusion, p-type $Bi_{0.4}Sb_{1.6}Te_3$ nanocomposites with enhanced figure of merit were obtained through a rapid and high yield processing method. The microstructures of the nanocomposites exhibited a wide variety of micronsized/nanosized particles, which aided in the effective scattering of phonons of a wide spectrum of wavelength. The slight reduction in power factor was hence compensated by the significant reduction in the thermal conductivities of the nanocomposites, resulting in the enhancement in the ZT values. A maximum ZT of 1.8 at 43 °C was obtained in the 40 wt % NC, the highest ZT obtained to date for p-type bismuth telluride based materials. By varying the weight percent of nanoinclusions and other processing conditions, the thermoelectric properties can be further fine-tuned to obtain an optimum ZT. This processing method can be extended to other materials systems and are scalable for mass production purposes.

This work is supported and funded by DSO National Laboratories, Singapore under Project No. DSOCL07135.

[1]T. Kerr, Combined Heat and Power- Evaluating the Benefits of Greater Global Investment (International Energy Agency, 2008), pp. 1–39, see http://www.iea.org/publications/free_new_Desc.asp?PUBS_ID=2010.
[2]T. M. Tritt, H. Bottner, and L. Chen, MRS Bull. **33**, 366 (2008).
[3]G. J. Snyder and E. S. Toberer, Nat. Mater. **7**, 105 (2008).
[4]L. D. Hicks and M. S. Dresselhaus, Phys. Rev. B **47**, 12727 (1993).
[5]R. Venkatasubramanian, E. Siivola, T. Colpitts, and B. O'uinn, Nature (London) **413**, 597 (2001).
[6]T. C. Harman, P. J. Taylor, M. P. Walsh, and B. E. LaForge, Science **297**, 2229 (2002).
[7]M.-S. Jeng, R. Yang, D. Song, and G. Chen, J. Heat Transfer **130**, 042410 (2008).
[8]A. J. Minnich, M. S. Dresselhaus, Z. F. Ren, and G. Chen, Energy Environ. Sci. **2**, 466 (2009).
[9]B. Poudel, Q. Hao, Y. Ma, Y. Lan, A. Minnich, B. Yu, X. Yan, D. Wang, A. Muto, D. Vashaee, X. Chen, J. Liu, M. S. Dresselhaus, G. Chen, and Z. Ren, Science **320**, 634 (2008).
[10]X. W. Wang, H. Lee, Y. C. Lan, G. H. Zhu, G. Joshi, D. Z. Wang, J. Yang, A. J. Muto, M. Y. Tang, J. Klatsky, S. Song, M. S. Dresselhaus, G. Chen, and Z. F. Ren, Appl. Phys. Lett. **93**, 193121 (2008).
[11]H. L. Ni, X. B. Zhao, T. J. Zhu, X. H. Ji, and J. P. Tu, J. Alloys Compd. **397**, 317 (2005).
[12]X. B. Zhao, X. H. Ji, Y. H. Zhang, T. J. Zhu, J. P. Tu, and X. B. Zhang, Appl. Phys. Lett. **86**, 062111 (2005).
[13]T. J. Zhu, F. Yan, X. B. Zhao, S. N. Zhang, Y. Chen, and S. H. Yang, J. Phys. D **40**, 6094 (2007).
[14]J. L. Mi, X. B. Zhao, T. J. Zhu, and J. P. Tu, J. Phys. D **41**, 205403 (2008).
[15]Y. Q. Cao, X. B. Zhao, T. J. Zhu, X. B. Zhang, and J. P. Tu, Appl. Phys. Lett. **92**, 143106 (2008).
[16]W. Xie, X. Tang, Y. Yan, Q. Zhang, and T. M. Tritt, Appl. Phys. Lett. **94**, 102111 (2009).
[17]X. Tang, W. Xie, H. Li, W. Zhao, and Q. Zhang, Appl. Phys. Lett. **90**, 012102 (2007).
[18]H. Li, X. Tang, X. Su, and Q. Zhang, Appl. Phys. Lett. **92**, 202114 (2008).
[19]B. C. Sales, D. Mandrus, B. C. Chakoumakos, V. Keppens, and J. R. Thompson, Phys. Rev. B **56**, 15081 (1997).
[20]Y. Lan, B. Poudel, Y. Ma, D. Wang, M. S. Dresselhaus, G. Chen, and Z. Ren, Nano Lett. **9**, 1419 (2009).